EXPERIMENTAL and MOLECULAR MEDICINE, Vol. 43, No. 1, 7-14, January 2011

# Microglial $P2X_7$ receptor expression is accompanied by neuronal damage in the cerebral cortex of the $APP_{swe}$/PS1dE9 mouse model of Alzheimer's disease

**Hwan Goo Lee[1,2,3], Sun Mi Won[1,5], Byoung Joo Gwag[1,4,5] and Yong Beom Lee[1,2,3,6]**

[1]Neuroscience Graduate Program
[2]Brain Disease Research Center
[3]Institute for Medical Science
[4]Department of Pharmacology
Ajou University School of Medicine
[5]Neurotech Pharmaceuticals Co. Ltd.
Suwon 443-721, Korea
[6]Corresponding author: Tel, 82-31-219-4558;
Fax, 82-31-219-4530; E-mail, yblee@ajou.ac.kr
DOI 10.3858/emm.2011.43.1.001

Accepted 18 November 2010
Available Online 19 November 2010

Abbreviations: AD, Alzheimer's disease; Aβ, β-amyloid peptide; fAβ, fibrillar Aβ; $P2X_7R$, $P2X_7$ receptor; PSD95, postsynaptic density 95; ROS, reactive oxygen species

## Abstract

**The possibility that $P2X_7$ receptor ($P2X_7R$) expression in microglia would mediate neuronal damage *via* reactive oxygen species (ROS) production was examined in the $APP_{swe}$/PS1dE9 mouse model of Alzheimer's disease (AD). $P2X_7R$ was predominantly expressed in CD11b-immunopositive microglia from 3 months of age before Aβ plaque formation. In addition, $gp91^{phox}$, a catalytic subunit of NADPH oxidase, and ethidium fluorescence were detected in $P2X_7R$-positive microglial cells of animals at 6 months of age, indicating that $P2X_7R$-positive microglia could produce ROS. Postsynaptic density 95-positive dendrites showed significant damage in regions positive for $P2X_7R$ in the cerebral cortex of 6 month-old mice. Taken together, up-regulation of $P2X_7R$ activation and ROS production in microglia are parallel with Aβ increase and correlate with synaptotoxicity in AD.**

**Keywords:** adenosine triphosphate; Alzheimer disease; amyloid β-protein precursor; Dlgh4 protein, mouse; microglia; reactive oxygen species; receptors, purinergic $P2X_7$

## Introduction

It has been hypothesized that amyloid β (Aβ) peptide, the major component of senile plaques, induces neurodegeneration in patients with Alzheimer's disease (Hardy and Selkoe, 2002). Several studies have found that the degree of aggregation of Aβ determines both Aβ toxicity and the nature of toxic manifestations (Pike *et al*., 1991; Eckman and Eckman, 2007). However, other reports have indicated that, in the brain of AD patients, there is a weak correlation between the severity of neuronal damage and plaque load (Lue *et al*., 1999; McLean *et al*., 1999). Accordingly, it has been suggested that soluble oligomeric Aβ mediates all of synaptic loss and dysfunction (Haass and Selkoe, 2007), and oxidative stress (Reddy, 2009), as early events in AD pathology.

Microglia are the major inflammatory cells of the brain, producing inflammatory cytokines and reactive oxygen species (ROS) in response to brain injury (Block, 2008; Perry *et al*., 2010). A consensus has emerged that downregulation of the clearance of Aβ and neurotoxins from activated microglia promote neuronal degeneration (Akiyama *et al*., 2000; McGeer and McGeer, 2002; Cameron and Landreth, 2010; Lue *et al*., 2010). In mixed neuron-microglia cultures, fibrillar Aβ (fAβ) stimulates microglia to produce superoxide by activating NADPH oxidase (Bianca *et al*., 1999), resulting in neurotoxicity (Qin *et al*., 2002). Activation of NADPH oxidase has also been detected in AD brains (Shimohama *et al*., 2000). Such findings suggest that microglia mediate the indirect cytotoxicity of Aβ by increasing the level of oxidative stress in the AD brain.

$P2X_7$ receptor ($P2X_7R$), one of the purinergic receptors, is an ATP-gated cation channel allowing $Ca^{2+}$ and $Na^+$ influx and $K^+$ efflux (Burnstock, 2007). Recently, $P2X_7R$ has been identified as an important element in neuroinflammation and neurodegeneration (Skaper *et al*., 2010). $P2X_7R$ induces interleukin-1β (IL-1β) release from microglia by the activation of IL-1β converting enzyme, mediated, in turn, by the efflux of $K^+$ from cells (Ferrari *et al*., 2006). In addition, prolonged activation of microglial $P2X_7R$ results in an increase in cytoplasmic $Ca^{2+}$ level, NADPH oxidase activation, and superoxide generation, resulting in neuronal injury upon

co-culture of neurons and microglia (Parvathenani *et al*., 2003; Skaper *et al*., 2006). Recently, it has been proposed that microglial $P2X_7R$ plays a role in the pathology of AD. Upregulation of $P2X_7R$ expression was seen both in microglia from AD human brains and in the microglia of Aβ-injected rat brains (McLarnon *et al*., 2006). However, the mechanisms responsible for Aβ-stimulated NADPH oxidase activation in the AD brain remain unclear. We have previously shown that ATP released from Aβ-stimulated microglia induced ROS production in culture *via* $P2X_7R$-mediated NADPH oxidase activation (Kim *et al*., 2007). This observation prompted us to study the possibility that Aβ-mediated $P2X_7R$ activation in microglia is associated with Aβ-caused neuronal injury in the AD brain. Characterization of the timing and nature of $P2X_7R$ activation during AD development is important to develop an understanding of disease progression. Hence, we here examined age-related $P2X_7R$ expression, ROS production in microglia, and neuronal damage, in the $APP_{swe}$/PS1dE9 (APP/PS1) mouse model of AD.

## Results

### Age-dependent Aβ accumulation and $P2X_7R$ expression

To correlate the $P2X_7R$ expression profile with the progress of AD pathogenesis, we first analyzed receptor expression in the cerebral cortex of APP/PS1 (Tg mice), from 1-12 months of age. Western blotting revealed a 75-kDa band corresponding to $P2X_7R$, and the protein levels in Tg mice rose significantly when the animals were 3-12 months of age, compared to age-matched non-Tg littermates. Notably, protein levels increased also in non-Tg mice 12 months of age (Figures 1A and B). Thus, $P2X_7R$ levels progressively rose with age, in line with the development of AD pathogenesis. In agreement with the Western blot data, double labeling with thioflavin-S and $P2X_7R$ revealed that $P2X_7R$ expression increased in parallel with accumulation of thioflavin-S-positive fibrillar Aβ (fAβ). Interestingly, $P2X_7R$ expression was evident from 3 months preceding Aβ plaque formation, and strong $P2X_7R$ immunostaining was noted not only around Aβ plaques but also in regions distant from such plaques (Figure 1C). These findings prompted us to investigate the identity of $P2X_7R$-expressing cells, and to seek to correlate the expression of $P2X_7R$ and Aβ both in the cores of plaques and also in regions where plaques were diffuse.

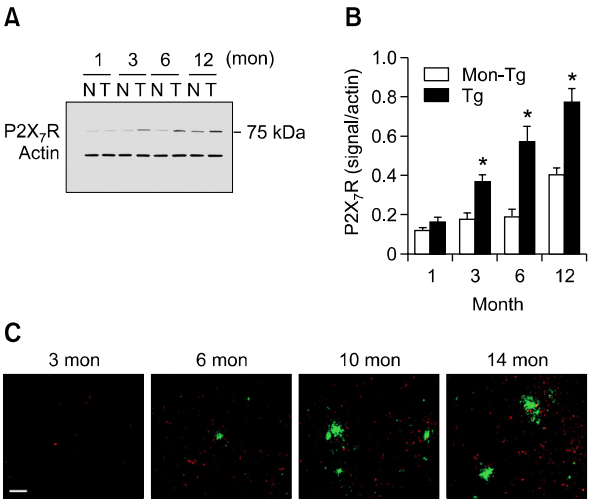


**Figure 1.** Aβ accumulation and $P2X_7R$ expression in APP/PS1 mice. (A) Western blot analysis of $P2X_7R$ and actin in the cerebral cortex from 1, 3, 6, and 12 month-old Tg mice and non-Tg control. (B) $P2X_7R$ levels were measured at indicated points of time, normalized to those of β-actin and presented as means ± SEM (n = 3 animals for each condition). $^*P < 0.01$ compared with age-matched non-Tg control, using ANOVA and Student-Newman-Keuls analyses. (C) Fluorescent photomicrographs of cerebral cortex section from 3, 6, 10, and 14 month-old Tg mouse labeled with the antibody against $P2X_7R$ and thioflavin-S. $P2X_7R$ (red) expression increased in parallel with accumulation of thioflavin-S-positive fibrillar Aβ (green). Abbreviations: N, non-Tg; T, Tg. Scale bar: 100 μm.

### $P2X_7R$ expression in CD11b-positive microglia

Triple immunofluorescence studies using antibodies against CD11b, $P2X_7R$, and $Aβ_{17-24}$ (4G8) were performed on brain sections from 3, 6, 10, and 14 month-old Tg mice. Double labeling with CD11b and $P2X_7R$ revealed that the vast majority of cortical cells showing $P2X_7R$ expression were CD11b-positive microglia, at both early and late timepoints. Double labeling with $P2X_7R$ and 4G8 showed that $P2X_7R$ immunostaining co-localized with microdeposits of Aβ both in the cores of plaques and in regions where plaques were diffuse, indicating that non-fibrillar Aβ-mediated $P2X_7R$ induction might occur in AD pathology. In support of this notion, triple labeling with CD11b, $P2X_7R$, and 4G8 showed a $P2X_7R$-negative microglial cell in contact with a plaque (Figure 2; from the brain of a 10 month-old mouse). In addition, the intensity of $P2X_7R$ staining increased with age, indicating that upregulation of $P2X_7R$ potentially played a role in AD progression (Figure 2). Additional experiment to quantify the co-localization of $P2X_7R$ in CD11b-postive cells in the frontal cortex and hippocampus was carried out, using 12 month-old Tg mice. The percentage of $P2X_7R^+$/$CD11b^+$ in total $P2X_7R^+$ cells was 88.8, 86.5, 70.1, and 79.1 % within the Layers III to V of frontal cortex, CA1 pyramidal layer, hilus, and granule cell

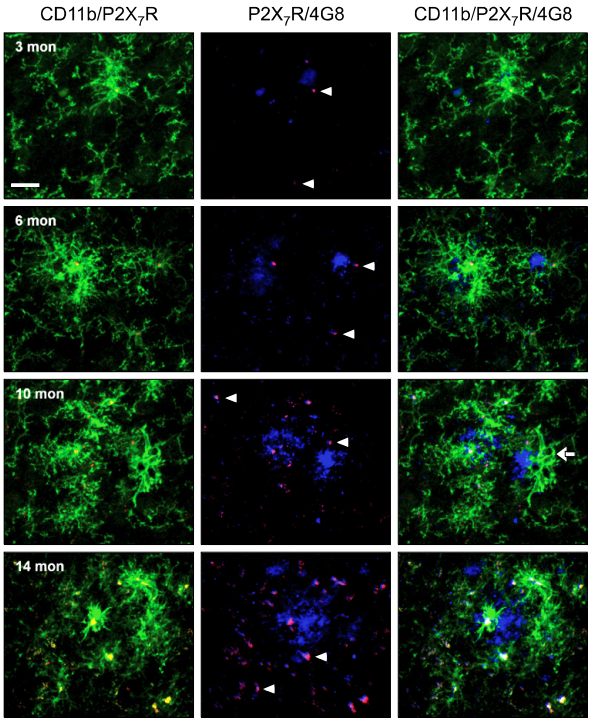


**Figure 2.** P2X$_7$R expression in CD11b-positive microglia. Fluorescent photomicrographs of the cerebral cortex from 3, 6, 10, and 14 month-old Tg mice labeled with antibodies against CD11b (green), P2X$_7$R (red) and A$\beta_{17\text{-}24}$ (4G8) (blue). Double labeling with CD11b and P2X$_7$R showed the P2X$_7$R expression in CD11b-positive microglia (yellow). P2X$_7$R immunostaining co-localized with microdeposits of Aβ (arrowheads). Triple labeling with CD11b, P2X$_7$R, and 4G8 showed a P2X$_7$R-negative microglial cell in contact with a plaque in the brain of a 10 month-old mouse (arrow). Scale bar: 20 μm.

layer of dentate gyrus respectively (see Table 1), indicating that major cell type showing P2X$_7$R expression is CD11b-positive microglia in the frontal cortex and hippocampus of AD brain. In addition, we also observed that 77.7% of cells showing P2X$_7$R expression were CD11b-positive microglia in the frontal cortex of 12 month-old non-Tg mice. These findings extend the previous studies showing the expression of P2X$_7$R in microglia around Aβ plaques in the late stage of a mouse model of AD, and in human AD autopsy brain tissue (Parvathenani *et al*., 2003; McLarnon *et al*., 2006) by providing a comprehensive spatial and temporal analysis.

## ROS production in P2X$_7$R-positive microglia

To correlate the ROS production profile with expression of P2X$_7$R, we analyzed the expression of the catalytic subunit of NADPH oxidase (gp91$^{phox}$) in the cerebral cortex of Tg mice 1-12 months of age. Western blot analysis revealed a 58-kDa band

**Table 1.** Colocalization of P2X$_7$R and CD11b in APP/PS1 Tg mice

| Frontal cortex | | Hippocampus | |
|---|---|---|---|
| Layer III to V | CA1 Layer | Hilus | DG Layer |
| 88.80 ± 8.00* | 86.49 ± 9.75 | 70.13 ± 9.53 | 79.14 ± 11.91 |

Age: 12 mon; *: percentage of P2X$_7$R$^+$/CD11b$^+$ in total P2X$_7$R$^+$ cells.

corresponding to gp91$^{phox}$, and the protein levels in Tg mice were significantly increased in the interval 6-12 months of age compared to age-matched non-Tg littermates ($P < 0.01$) (Figures 3A and B). Notably, the time course of gp91$^{phox}$ expression was similar to the kinetics of P2X$_7$R expression, which began to rise 3 months before gp91$^{phox}$ was detected. To confirm that P2X$_7$R-positive microglia could produce ROS at early stage of AD progression, triple labeling using either antibodies against CD11b, P2X$_7$R, and gp91$^{phox}$; or antibodies against CD11b and P2X$_7$R, and the chemical hydroethidine (HE); were performed on brain sections of 6 month-old Tg mice. Triple labeling with CD11b, P2X$_7$R, and gp91$^{phox}$ showed that most gp91$^{phox}$ staining could be merged with P2X$_7$R-positive microglia. Finally, triple labeling with CD11b, P2X$_7$R, and HE showed that P2X$_7$R-positive microglia was merged with ethidium fluorescence, indicating that P2X$_7$R-positive microglia could produce ROS in the Tg mouse model of AD (Figure 3C).

## Postsynaptic density loss with P2X$_7$R-positive microglia

It is known that synapse loss occurs in AD brains, and an association of Aβ peptides with dendritic spine loss and reductions in the levels of postsynaptic scaffold proteins, such as postsynaptic density-95 (PSD95) protein, have been observed in mouse models of AD (Pham *et al*., 2010). To determine the time point of PSD loss in Tg mice, we analyzed the levels of PSD95 in the cerebral cortex of Tg mice 1-12 months of age. Western blot analysis revealed a 95-kDa band corresponding to PSD95, and the protein levels in Tg mice were significantly decreased in the interval 6-12 months of age compared to age-matched non-Tg littermates ($P < 0.01$) (Figures 4A and B). To test whether ROS released from Aβ-stimulated microglia *via* P2X$_7$R activation correlates with synapse loss, immunofluorescence studies using antibodies against PSD95, P2X$_7$R, and A$\beta_{17\text{-}24}$ (4G8) were performed on brain sections from 6 and 12 month-old Tg mice. First, the density of PSD95 staining in brain sections from such animals

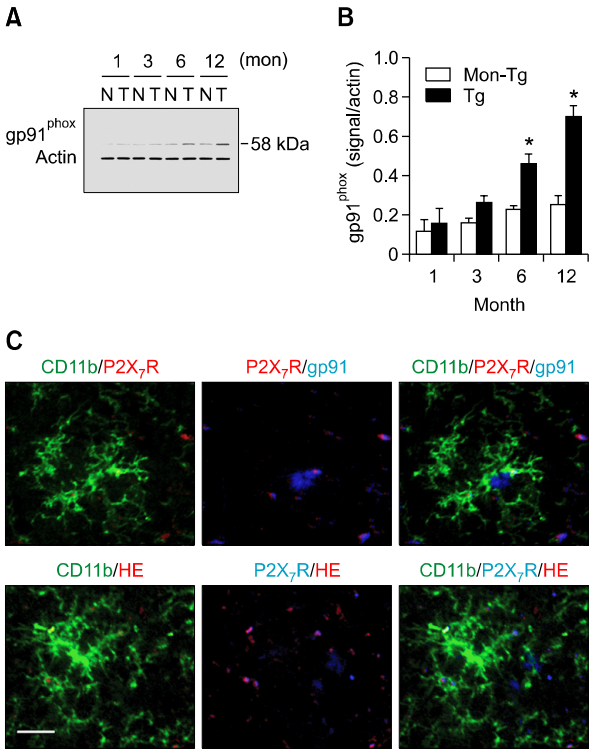


**Figure 3.** Gp91$^{phox}$ expression and ROS production in P2X$_7$R-positive microglia. (A) Western blot analysis of gp91$^{phox}$ and actin in the cerebral cortex from 1, 3, 6, and 12 month-old Tg mice and non-Tg control. (B) gp91$^{phox}$ levels were measured at indicated points of time, normalized to those of β-actin and presented as means ± SEM (n = 3 animals for each condition). *$P < 0.01$ compared with age-matched non-Tg control, using ANOVA and Student-Newman-Keuls analyses. (C) Fluorescent photomicrographs of cerebral cortex sections of 6 month-old Tg mice immunolabeled with either antibodies against CD11b (green), P2X$_7$R (red), and gp91$^{phox}$ (blue) or antibodies against CD11b (green) and P2X$_7$R (blue), and the chemical hydroethidine (HE) (red). Abbreviations: N, non-Tg; T, Tg. Scale bar: 20 μm.

appeared to be reduced (Figure 4C, b, c) compared to that in 6 month-old control section (Figure 4C, a). Overall, the PSD95 loss profile was closely associated with P2X$_7$R expression (Figure 4C, b, c). Red spots indicating P2X$_7$R were correlated with sparse PSD95 staining, dendritic dystrophy, and neuronal cell body atrophy at 6 months (Figure 4C, b2), and such neuronal damages were augmented with increase of P2X$_7$R expression at 12 months (Figure 4C, c3).

## Discussion

Although it has been proposed that activated microglia surrounding amyloid plaques cause neurodegeneration by producing neurotoxins (Akiyama *et al*., 2000; McGeer and McGeer, 2002), the mechanisms underlying microglia-mediated neuronal damage in the AD brain remain to be elucidated. In the present study, we observed that P2X$_7$R expression and ROS production in Aβ-stimulated microglia were tightly associated with Aβ-mediated synapse loss in a mouse model of AD.

Here, we show that microglia were the major cell type demonstrating P2X$_7$R-immunopositivity in the cerebral cortex of Tg mouse model of AD. Moreover, P2X$_7$R expression was observed before Aβ plaque formation, and evident in regions with diffuse plaques, suggesting that non-fibrillar Aβ may be sufficient for P2X$_7$R induction. Recently, soluble oligomers of Aβ have been suggested as potent stimulators of microglial activation (Hashioka *et al*., 2005; Jimenez *et al*., 2008), although most studies have considered fAβ to be a more powerful stimulus (McDonald *et al*., 1997; Combs *et al*., 2001). These findings suggest that P2X$_7$R expression in microglia can be induced by soluble Aβ even very early in the course of AD pathogenesis. The ability of oligomeric Aβ to activate microglia provides crucial evidence that a soluble intermediate form of Aβ may cause oxidative damage prior to plaque formation in both humans and animal AD models (Pratico *et al*., 2001; Sonnen *et al*., 2008). Moreover, positron emission tomography studies of living AD patients, using the ligand PK11195, which specifically identifies activated microglia, have shown that microglial activation is evident even at early stages of the disease (Cagnin *et al*., 2001; Okello *et al*., 2009). Our finding that P2X$_7$R expression precedes Aβ plaque formation strengthens this view. Moreover, a recent study demonstrated that overexpression of P2X$_7$R alone, in the absence of any pathological insult, was sufficient to drive the activation and proliferation of microglia in rat primary hippocampal cultures (Monif *et al*., 2009). On the while, we observed minor population of P2X$_7$R$^+$/CD11b$^-$ cells in the frontal cortex and hippocampal areas of 12 month-old Tg mice, and recent study reported the altered neuronal expression of P2X$_7$R in mouse models of Huntington's disease (Diaz-Hernández *et al*., 2009). Therefore, we can not rule out the possibility that P2X$_7$R expression in other cell types including neuron is involved in the pathogenesis of AD.

Although it is unclear whether the production of inflammatory mediators in the AD brain enhances or retards disease progression, ROS synthesized by NADPH oxidase have been shown to mediate both Aβ-induced neuronal damage in co-cultures of neurons and microglia (Qin *et al*., 2002) and Aβ-caused cerebrovascular dysfunction (Park *et al*., 2005). As evidence that P2X$_7$R is the missing link between Aβ and ROS production, ATP re-

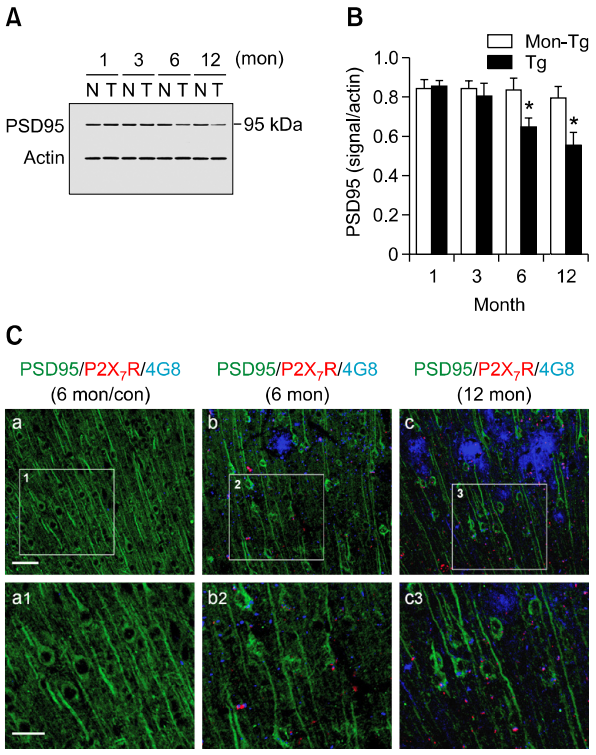


**Figure 4.** Microglial P2X$_7$R expression and their association with PSD loss in APP/PS1 mice. (A) Western blot analysis of PSD95 and actin in the cerebral cortex from 1, 3, 6, and 12 month-old Tg mice and non-Tg control. (B) PSD95 levels were measured at indicated points of time, normalized to those of β-actin and presented as means ± SEM (n = 3 animals for each condition). *$P < 0.01$ compared with age-matched non-Tg control, using ANOVA and Student-Newman-Keuls analyses. (C) Fluorescent photomicrographs of cerebral cortex sections of 6- and 12-month-old APP/PS1 (b, c) and 6-month-old non-Tg mice (a) immunolabeled with antibodies against PSD95 (green), P2X$_7$R (red), and Aβ$_{17-24}$ (4G8) (blue). a1, b2, and c3 are higher magnification images of the areas designated in a, b, and c. Abbreviations: N, non-Tg; T, Tg. Scale bars: a-f, 50 μm; a1-c3, 15 μm.

leased from Aβ-stimulated microglia induced ROS production in culture *via* P2X$_7$R-mediated NADPH oxidase activation (Kim *et al*., 2007), and a recent study showed that intrahippocampal injection of Aβ caused IL-1β accumulation in wild-type brain but not in that of P2X$_7$R knock-out mice (Sanz *et al*., 2009). In the present study, Western blot analysis and triple immunostaining for CD11b, P2X$_7$R, and gp91$^{phox}$ demonstrated that gp91$^{phox}$ expression and ROS production increased significantly from 6 months of age in the P2X$_7$R-positive microglia (Figure 3). These results indicate that Aβ-stimulated microglia may be involved in the development of oxidative stress even during the early stages of AD, by inducing and activating P2X$_7$R. In support of our findings, a recent study observed a sudden elevation in protein oxidation and lipid peroxidation in brains of APP/PS1 mice at about 6 months of age (Abdul *et al*., 2008).

Recently, the potential role played by neurotoxic Aβ oligomers in AD pathology has encouraged the development of a modified amyloid hypothesis. Soluble forms of Aβ induce synaptic damage and dendritic spine loss, and levels of synaptic proteins, including the presynaptic protein synaptophysin and the postsynaptic protein PSD95, are decreased in the AD brain (Gylys *et al*., 2004; Reddy *et al*., 2005). However, the detailed mechanisms of how Aβ causes such synaptic changes remain unclear. A recent report found that oligomeric Aβ surrounding plaques contributed to excitatory synapse loss in a mouse model of AD, and suggested that oligomeric Aβ may interact directly with synaptic proteins to cause dysfunction and eventual spine collapse (Koffie *et al*., 2009). On the other hand, recent studies found that oxidative stress was principally localized to synapses of the frontal cortex in the AD brain (Ansari and Scheff, 2010), and that microglia expressed high levels of gp91$^{phox}$ in a vulnerable brain region of mild cognitive impairment (MCI) patients (Bruce-Keller *et al*., 2010). In this regard, we found that cerebral cortex samples of Tg mice aged 6 months showed significant damage to PSD95-immunoreactive dendrites in regions staining positively for P2X$_7$R (Figure 4). This finding suggests that P2X$_7$R-positive microglia-mediated oxidative stress may cause synaptic loss. Moreover, we observed that most P2X$_7$R and 4G8 immunostaining of Aβ co-localized (Figure 2). Therefore, our present work suggests that P2X$_7$R-mediated ROS production in Aβ-stimulated microglia is one mechanism explaining oligomeric Aβ-mediated synaptotoxicity. Even though correlational studies such as the present work can only suggest contributions of microglial Aβ stimulation and synapse loss to AD pathology, recent studies in support of this hypothesis have shown that microglial activation and hippocampal synapse loss preceded tangle formation in the *tau* Tg mouse (Yoshiyama *et al*., 2007), and that inflammation triggered synaptic degeneration in mice with experimental autoimmune encephalomyelitis, an animal model of multiple sclerosis (Centonze *et al*., 2009). Interestingly, brain sections of 12 month-old non-Tg mice showed that the majority of cells showing P2X$_7$R expression were CD11b-positive microglia. Microglial activation in healthy aging brain and the possibility of involvement in neuronal loss and decline of cognitive function have been reported (Sheng *et al*., 1998; Cagnin *et al*., 2001). These imply that microglial P2X$_7$R expression in AD might be influenced to some extent by other aging factors besides Aβ, and contribute to AD pathology.

Together, the results suggest that Aβ-stimulated microglia may induce excessive production of ROS *via* the action of $P2X_7R$, leading to neuronal damage even at early stages of AD pathogenesis, which may help to explain how microglia mediate neuronal damage in the AD brain.

## Methods

### Transgenic mouse model

Double transgenic mice expressing a chimeric mouse/human amyloid precursor protein (Mo/HuAPP695swe) and a mutant human presenilin 1 (PS1-dE9) was obtained from Jackson Laboratory (Bar Harbor, ME) and maintained by crossing transgenic males with C57BL/6J × C3H/HeJ F1 female mice from Jackson Laboratory. APP/PS1 mice carry mouse APP with the double mutations (K595N and M596L) and human PS1 with a deletion of exon 9 found in familial AD patients. APP/PS1 mice used were 1-14 months old. For each experimental group, 3-4 female mice were used. All animal procedures were performed in accordance with the guidelines of the Institutional Animal Care and Use Committee of Ajou University School of Medicine.

### Tissue preparation and immunohistochemistry

Animals were transcardially perfused with a saline solution containing 0.5% sodium nitrate and heparin (10 U/ml) followed by 4% paraformaldehyde dissolved in 0.1 M phosphate buffer (PB). Brains were removed from the cranium and postfixed for 1 h at 4°C, washed in 0.1 M PB and then immersed in 30% sucrose solution until they sank. Tissues were sectioned on a sliding microtome at a thickness of 35 μm, and then stored in stock solution [0.1 M phosphate buffer (pH 7.4), 30% (v/v) glycerol, 30% ethylene glycol] at 4°C until use. Serial brain section was selected and processed for immunostaining as described previously (Wang *et al*., 2008). In brief, brain sections were incubated in PBS containing 0.2% Triton X-100 and 0.5% bovine serum albumin (BSA) for 30 min at room temperature (RT), rinsed two times in PBS containing 0.5% BSA, and then incubated overnight at 4°C with the appropriate primary antibodies: rat anti CD11b (1:200; Serotec, Oxford, UK), rabbit anti $P2X_7$ receptor (1:200; Sigma, St. Louis, MO), goat anti $P2X_7$ receptor (1:200; Santacruz Biotechnology, Santa Cruz, CA), mouse monoclonal 4G8 (amino acids 17-24 of Aβ peptide, 1:200; Covance, Emeryville, CA), mouse anti $gp91^{phox}$ (1:200; BD Biosciences, San Diego, CA), or rabbit anti PSD95 (1:200; Abcam, Cambridge, UK). After incubation, sections were rinsed three times for 5 min in PBS and subsequently incubated with the corresponding secondary antibodies: FITC-labeled anti-rabbit IgG (1:200; Invitrogen, Carlsbad, CA), FITC-labeled anti-rat IgG (1:200; Invitrogen), Texas Red-labeled anti-rabbit IgG (1:200; Vector, Burlingame, CA), Texas Red-labeled anti-goat IgG (1:200; Invitorgen), AMCA-labeled anti-mouse IgG. (1:200; Vector), or AMCA-labeled anti-rabbit IgG. (1:200; Vector) for 2 h at RT. Tissues were mounted with Vectashield mounting medium (Biomed Corp., Foster City, CA) and viewed using an Olympus IX71 confocal laser scanning microscope (Olympus; Tokyo, Japan).

### Thioflavin S staining

For thioflavin S staining, brain sections were mounted on gelatine-coated slides. After drying, slides were rinsed with water and incubated with thioflavin S (1% w/v; Sigma) for 5 min. Subsequently slides were rinsed in 70% ethanol for 5 min and briefly rinsed in water. For combination with $P2X_7$ receptor (1:200; Sigma) immunofluorescence staining, sections were first fluorescence labeled as described above and subsequently stained with thioflavin S.

### Counting of $P2X_7R^+/CD11b^+$ cells

The percentage of $P2X_7R^+/CD11b^+$ in total $P2X_7R^+$ cells within the Layers III to V of frontal cortex and hippocampus including CA1 pyramidal layer, hilus, and granule cell layer of dentate gyrus was quantified by counting the cells within a 250 × 250 μm square box, using an IX71 confocal laser scanning microscope (Olympus) at a magnification of 400 ×. The mean number of $P2X_7R^+/CD11b^+$ cells was calculated from five areas of each section from 3 animals.

### *In situ* detection of $O_2^-$ and $O_2^-$-derived oxidants

Hydroethidine histochemistry was performed for *in situ* visualization of $O_2^-$ and $O_2^-$-derived oxidants (Wu *et al*., 2003). Hydroethidine (1 mg/ml in PBS containing 1% dimethylsulfoxide; Molecular Probes, Eugene, OR) was administered intraperitoneally. After 15 min, brain sections were prepared and mounted on gelatin-coated slides, and the oxidized hydroethidine product, ethidium, was examined by confocal microscopy (Olympus).

### Western blot analysis

Cerebral cortex tissues were isolated from transgenic mice and age-matched non-transgenic littermates at each time point. Tissues were homogenized with ice-cold lysis buffer containing 50 mM Tris-HCl pH 7.5, 150 mM NaCl, 2 mM EDTA, 0.1% SDS, 0.5% sodium deoxycholate, supplemented with a protease inhibitors cocktail (Sigma). The homogenate was then centrifuged at 13,000 × *g* for 10 min and the supernatants collected. Protein concentration was determined using the DC protein assay kit (Bio-Rad, Hercules, CA). Total protein (40 μg) from each sample was separated on a 10% sodium dodecyl sulfate polyacrylamide gel electrophoresis (SDS-PAGE) gel and transferred to polyvinylidene difluoride (PVDF) membranes (Millipore, Bedford, MA). After transfer, membranes were incubated in blocking buffer [tris-buffered saline (TBS) containing 0.5% skim milk] for 1 h at RT and then incubated overnight at 4°C with following primary antibodies: rabbit anti $P2X_7$ receptor (1:500; Sigma), mouse anti $gp91^{phox}$ (1:1000; BD Biosciences), rabbit anti PSD95 (1:1000; Abcam), and monoclonal anti β-actin (1:5000; Sigma). After several washes in 0.1% Tween-20 (Sigma) in TBS, membranes were incubated with the corresponding HRP-conjugated secondary antibodies (Amersham Biosciences, Bucking-

hamshire, UK) for 1 h at RT. After washing, blots were developed with ECL detection reagents (Amersham Biosciences), and exposed to X-ray film. The average intensity value of the pixels in a background selected region was calculated and was subtracted from each pixel in the samples using IamgeQuant software (Image Guage 4.0; Fuji Film, Tokyo, Japan). The densitometry values obtained were normalized with respect to the values obtained with anti-β-actin to ascertain the same amount of protein.

### Statistical analysis

All values are represented as mean ± SEM. Statistical significance ($P < 0.05$ for all analyses) was assessed by analysis of variance (ANOVA) using Instat 3.05 (GraphPad Software, San Diego, CA), followed by Student-Newman-Keuls analyses.

### Acknowledgements

This work was supported by the Brain Korea 21 Project for Medical Science, Ajou University, and Neurotech Pharmaceuticals.

## References

Abdul HM, Sultana R, St Clair DK, Markesbery WR, Butterfield DA. Oxidative damage in brain from human mutant APP/PS-1 double knock-in mice as a function of age. Free Radic Biol Med 2008;45:1420-5

Akiyama H, Barger S, Barnum S, Bradt B, Bauer J, Cole GM, Cooper NR, Eikelenboom P, Emmerling M, Fiebich BL, Finch CE, Frautschy S, Griffin WS, Hampel H, Hull M, Landreth G, Lue L, Mrak R, Mackenzie IR, McGeer PL, O'Banion MK, Pachter J, Pasinetti G, Plata-Salaman C, Rogers J, Rydel R, Shen Y, Streit W, Strohmeyer R, Tooyoma I, Van Muiswinkel FL, Veerhuis R, Walker D, Webster S, Wegrzyniak B, Wenk G, Wyss-Coray T. Inflammation and Alzheimer's disease. Neurobiol Aging 2000;21:383-421

Ansari MA, Scheff SW. Oxidative stress in the progression of Alzheimer disease in the frontal cortex. J Neuropathol Exp Neurol 2010;69:155-67

Bianca VD, Dusi S, Bianchini E, Dal Pra I, Rossi F. Beta-amyloid activates the O-2 forming NADPH oxidase in microglia, monocytes, and neutrophils. A possible inflammatory mechanism of neuronal damage in Alzheimer's disease. J Biol Chem 1999;274:15493-9

Block ML. NADPH oxidase as a therapeutic target in Alzheimer's disease. BMC Neurosci 2008;9 Suppl 2:S8

Bruce-Keller AJ, Gupta S, Parrino TE, Knight AG, Ebenezer PJ, Weidner AM, LeVine H 3rd, Keller JN, Markesbery WR. NOX activity is increased in mild cognitive impairment. Antioxid Redox Signal 2010;12:1371-82

Burnstock G. Physiology and pathophysiology of purinergic neurotransmission. Physiol Rev 2007;87:659-797

Cagnin A, Brooks DJ, Kennedy AM, Gunn RN, Myers R, Turkheimer FE, Jones T, Banati RB. *In vivo* measurement of activated microglia in dementia. Lancet 2001;358:461-7

Cameron B, Landreth GE. Inflammation, microglia, and Alzheimer's disease. Neurobiol Dis 2010;37:503-9

Centonze D, Muzio L, Rossi S, Cavasinni F, De Chiara V, Bergami A, Musella A, D'Amelio M, Cavallucci V, Martorana A, Bergamaschi A, Cencioni MT, Diamantini A, Butti E, Comi G, Bernardi G, Cecconi F, Battistini L, Furlan R, Martino G. Inflammation triggers synaptic alteration and degeneration in experimental autoimmune encephalomyelitis. J Neurosci 2009;29:3442-52

Combs CK, Karlo JC, Kao SC, Landreth GE. Beta-Amyloid stimulation of microglia and monocytes results in TNFalpha-dependent expression of inducible nitric oxide synthase and neuronal apoptosis. J Neurosci 2001;21:1179-88

Diaz-Hernandez M, Diez-Zaera M, Sanchez-Nogueiro J, Gomez-Villafuertes R, Canals JM, Alberch J, Miras-Portugal MT, Lucas JJ. Altered P2X7-receptor level and function in mouse models of Huntington's disease and therapeutic efficacy of antagonist administration. FASEB J 2009;23:1893-906

Eckman CB, Eckman EA. An update on the amyloid hypothesis. Neurol Clin 2007;25:669-82

Ferrari D, Pizzirani C, Adinolfi E, Lemoli RM, Curti A, Idzko M, Panther E, Di Virgilio F. The P2X7 receptor: a key player in IL-1 processing and release. J Immunol 2006;176:3877-83

Gylys KH, Fein JA, Yang F, Wiley DJ, Miller CA, Cole GM. Synaptic changes in Alzheimer's disease: increased amyloid-beta and gliosis in surviving terminals is accompanied by decreased PSD-95 fluorescence. Am J Pathol 2004;165:1809-17

Haass C, Selkoe DJ. Soluble protein oligomers in neurodegeneration: lessons from the Alzheimer's amyloid beta-peptide. Nat Rev Mol Cell Biol 2007;8:101-12

Hardy J, Selkoe DJ. The amyloid hypothesis of Alzheimer's disease: progress and problems on the road to therapeutics. Science 2002;297:353-6

Hashioka S, Monji A, Ueda T, Kanba S, Nakanishi H. Amyloid-beta fibril formation is not necessarily required for microglial activation by the peptides. Neurochem Int 2005;47:369-76

Jimenez S, Baglietto-Vargas D, Caballero C, Moreno-Gonzalez I, Torres M, Sanchez-Varo R, Ruano D, Vizuete M, Gutierrez A, Vitorica J. Inflammatory response in the hippocampus of PS1M146L/APP751SL mouse model of Alzheimer's disease: age-dependent switch in the microglial phenotype from alternative to classic. J Neurosci 2008;28:11650-61

Kim SY, Moon JH, Lee HG, Kim SU, Lee YB. ATP released from beta-amyloid-stimulated microglia induces reactive oxygen species production in an autocrine fashion. Exp Mol Med 2007;39:820-7

Koffie RM, Meyer-Luehmann M, Hashimoto T, Adams KW, Mielke ML, Garcia-Alloza M, Micheva KD, Smith SJ, Kim ML, Lee VM, Hyman BT, Spires-Jones TL. Oligomeric amyloid

beta associates with postsynaptic densities and correlates with excitatory synapse loss near senile plaques. Proc Natl Acad Sci USA 2009;106:4012-7

Lue LF, Kuo YM, Roher AE, Brachova L, Shen Y, Sue L, Beach T, Kurth JH, Rydel RE, Rogers J. Soluble amyloid beta peptide concentration as a predictor of synaptic change in Alzheimer's disease. Am J Pathol 1999;155:853-62

Lue LF, Kuo YM, Beach T, Walker DG. Microglia activation and anti-inflammatory regulation in Alzheimer's disease. Mol Neurobiol 2010;41:115-28

McDonald DR, Brunden KR, Landreth GE. Amyloid fibrils activate tyrosine kinase-dependent signaling and superoxide production in microglia. J Neurosci 1997;17:2284-94

McGeer PL, McGeer EG. Local neuroinflammation and the progression of Alzheimer's disease. J Neurovirol 2002;8: 529-38

McLarnon JG, Ryu JK, Walker DG, Choi HB. Upregulated expression of purinergic P2X(7) receptor in Alzheimer disease and amyloid-beta peptide-treated microglia and in peptide-injected rat hippocampus. J Neuropathol Exp Neurol 2006;65:1090-7

McLean CA, Cherny RA, Fraser FW, Fuller SJ, Smith MJ, Beyreuther K, Bush AI, Masters CL. Soluble pool of Abeta amyloid as a determinant of severity of neurodegeneration in Alzheimer's disease. Ann Neurol 1999;46:860-6

Monif M, Reid CA, Powell KL, Smart ML, Williams DA. The P2X7 receptor drives microglial activation and proliferation: a trophic role for P2X7R pore. J Neurosci 2009;29:3781-91

Okello A, Edison P, Archer HA, Turkheimer FE, Kennedy J, Bullock R, Walker Z, Kennedy A, Fox N, Rossor M, Brooks DJ. Microglial activation and amyloid deposition in mild cognitive impairment: a PET study. Neurology 2009;72: 56-62

Park L, Anrather J, Zhou P, Frys K, Pitstick R, Younkin S, Carlson GA, Iadecola C. NADPH-oxidase-derived reactive oxygen species mediate the cerebrovascular dysfunction induced by the amyloid beta peptide. J Neurosci 2005; 25:1769-77

Parvathenani LK, Tertyshnikova S, Greco CR, Roberts SB, Robertson B, Posmantur R. P2X7 mediates superoxide production in primary microglia and is up-regulated in a transgenic mouse model of Alzheimer's disease. J Biol Chem 2003;278:13309-17

Perry VH, Nicoll JA, Holmes C. Microglia in neurodegenerative disease. Nat Rev Neurol 2010;6:193-201

Pham E, Crews L, Ubhi K, Hansen L, Adame A, Cartier A, Salmon D, Galasko D, Michael S, Savas JN, Yates JR, Glabe C, Masliah E. Progressive accumulation of amyloid-beta oligomers in Alzheimer's disease and in amyloid precursor protein transgenic mice is accompanied by selective alterations in synaptic scaffold proteins. FEBS J 2010; 277:3051-67

Pike CJ, Walencewicz AJ, Glabe CG, Cotman CW. Aggregation-related toxicity of synthetic beta-amyloid protein in hippocampal cultures. Eur J Pharmacol 1991;207:367-8

Pratico D, Uryu K, Leight S, Trojanoswki JQ, Lee VM. Increased lipid peroxidation precedes amyloid plaque formation in an animal model of Alzheimer amyloidosis. J Neurosci 2001;21:4183-7

Qin L, Liu Y, Cooper C, Liu B, Wilson B, Hong JS. Microglia enhance beta-amyloid peptide-induced toxicity in cortical and mesencephalic neurons by producing reactive oxygen species. J Neurochem 2002;83:973-83

Reddy PH, Mani G, Park BS, Jacques J, Murdoch G, Whetsell W Jr, Kaye J, Manczak M. Differential loss of synaptic proteins in Alzheimer's disease: implications for synaptic dysfunction. J Alzheimers Dis 2005;7:103-17; discussion 173-80

Reddy PH. Amyloid beta, mitochondrial structural and functional dynamics in Alzheimer's disease. Exp Neurol 2009;218:286-92

Sanz JM, Chiozzi P, Ferrari D, Colaianna M, Idzko M, Falzoni S, Fellin R, Trabace L, Di Virgilio F. Activation of microglia by amyloid {beta} requires P2X7 receptor expression. J Immunol 2009;182:4378-85

Sheng JG, Mrak RE, Griffin WS. Enlarged and phagocytic, but not primed, interleukin-1 alpha-immunoreactive microglia increase with age in normal human brain. Acta Neuropathol 1998;95:229-34

Shimohama S, Tanino H, Kawakami N, Okamura N, Kodama H, Yamaguchi T, Hayakawa T, Nunomura A, Chiba S, Perry G, Smith MA, Fujimoto S. Activation of NADPH oxidase in Alzheimer's disease brains. Biochem Biophys Res Commun 2000;273:5-9

Skaper SD, Facci L, Culbert AA, Evans NA, Chessell I, Davis JB, Richardson JC. P2X(7) receptors on microglial cells mediate injury to cortical neurons *in vitro*. Glia 2006;54: 234-42

Skaper SD, Debetto P, Giusti P. The P2X7 purinergic receptor: from physiology to neurological disorders. FASEB J 2010;24:337-45

Sonnen JA, Breitner JC, Lovell MA, Markesbery WR, Quinn JF, Montine TJ. Free radical-mediated damage to brain in Alzheimer's disease and its transgenic mouse models. Free Radic Biol Med 2008;45:219-30

Wang HK, Park UJ, Kim SY, Lee JH, Kim SU, Gwag BJ, Lee YB. Free radical production in CA1 neurons induces MIP-1alpha expression, microglia recruitment, and delayed neuronal death after transient forebrain ischemia. J Neurosci 2008;28:1721-7

Wu DC, Teismann P, Tieu K, Vila M, Jackson-Lewis V, Ischiropoulos H, Przedborski S. NADPH oxidase mediates oxidative stress in the 1-methyl-4-phenyl-1,2,3,6-tetrahydropyridine model of Parkinson's disease. Proc Natl Acad Sci USA 2003;100:6145-50

Yoshiyama Y, Higuchi M, Zhang B, Huang SM, Iwata N, Saido TC, Maeda J, Suhara T, Trojanowski JQ, Lee VM. Synapse loss and microglial activation precede tangles in a P301S tauopathy mouse model. Neuron 2007;53:337-51